Polymer Bulletin (2021) 78:1771–1795
https://doi.org/10.1007/s00289-020-03183-7

ORIGINAL PAPER

Study and modeling of thermomechanical properties of jute and Alfa fiber-reinforced polymer matrix hybrid biocomposite materials

Benabdellah Benyamina[1,2] · Allel Mokaddem[3] · Bendouma Doumi[1,3] · Mohammed Belkheir[3] · Mohammed Elkeurti[2]

Received: 24 July 2019 / Revised: 16 March 2020 / Accepted: 23 March 2020 / Published online: 2 April 2020

Abstract

In this paper, we have investigated and studied the effect of thermal stress on the fiber–matrix interface damage of three new hybrid biocomposite and biocomposite materials. Our genetic simulation based on Weibull probabilistic models showed that the jute–Alfa/PEEK (PEEK: thermoplastic matrix—polyetheretherketone) hybrid biocomposite material is more resistant to the mechanical and thermal stress applied comparing with the other biocomposites such as jute/PEEK and Alfa/PEEK with the same volume fraction used in our genetic model. Our results also show that natural fibers improve the physical properties of biocomposite materials, especially hybrid biocomposite materials. This finding is similar to that found by Antoine Le Duigou et al. where they have shown experimentally that the natural reinforcements greatly improve the properties of composite materials and also they have a very low environmental impact.

Keywords Jute · Alfa · Damage · Interface · Biocomposite · PEEK · Thermal stress · Genetic algorithm

✉ Allel Mokaddem
mokaddem.allel@gmail.com

✉ Bendouma Doumi
bdoummi@yahoo.fr

[1] Physics Department, Faculty of Science, University Dr. Tahar Moulay of Saida, Saida, Algeria

[2] Laboratory of Physico-Chemical Studies, University of Saida, 20000 Saida, Algeria

[3] Laboratoire d'Instrumentation et Matériaux Avancés, Centre Universitaire Nour Bachir El-Bayadh, BP 900 route Aflou, 32000 El Bayadh, Algeria

Introduction

A composite material consists of at least two components, a reinforcement and matrix. The composite materials are light and resistant compared to traditional materials. Biocomposite materials based on natural fibers have better physical properties compared to composite materials and respond favorably to environmental requirements due to their biodegradability and recycling characteristics.

The biocomposites are composite materials which comprise one or more phases from a biological origin [1, 2]. The reinforcing phase in most cases is derived from plant fibers in crops such as cotton, flax, or hemp, or from recycled wood, waste paper, crop-processing by-products, or regenerated cellulose fibers such as sisal, starch, and viscose/rayon. The matrix phase within a biocomposite may often take the form of a natural polymer, possibly derived from vegetable oils or starches. More commonly, however, synthetic fossil-derived polymers (recycled thermoplastics) act as the matrices [2]; among the natural fibers, we find the fiber Alfa and the jute fiber. The jute fiber is obtained from the bark of the jute. It is long, soft, and brilliant and is used among other things to make jute bags or as geotextile. The word jute refers to both the fibers and the plant from which they come [3].

The Alfa fiber (Fig. 1) is the Arabic name of the plant stipa tenacissima. It is a typical Mediterranean perennial; it grows in clumps of about 1 to 1.20 m high, thus forming large layers. It is widely distributed and grows spontaneously in arid and semiarid regions in northwestern Africa and southern Spain [4–7].

The stem of this plant is used in the industry of ropes and carpets. Also, the fiber of this plant is mainly used in the production of paper, in composites and nonwovens.

In Algeria, large Alfa requirements are destined for paper mills and estimated at 200,000 tons/year and national production amounts to 70,000 tons/year [8, 9].

Fig. 1 Illustration of the plant of Alfa in the raw state

In general, the tensile mechanical properties of technical Alfa approach those of jute, flax, hemp, and sisal [4–6].

The properties of composite and biocomposite materials are not limited to those of fiber and matrix but also take into account the quality of the fiber–matrix interface. Indeed, this interface has a vital role in transmitting the forces between the fibers and the matrix during a mechanical stress; if this interfacial adhesion is very strong at the microscopic scale, we will have a composite material with very important and interesting mechanical characteristics [10].

This interface initially depends on the wettability, when the melted matrix and the fiber are brought into contact, but also on the adhesion once the fiber–matrix system is in the solid state. For composite materials, the fiber–matrix adhesion with thermosetting resins is essentially by chemical bonds, whereas the adhesion phenomenon with a thermoplastic matrix appears mainly through to the physical interactions [10–12].

The adhesion is the parameter that characterizes the quality of the fiber–matrix interface at the solid scale (damaged and undamaged interface). The multiscale studies (folds and REV: representative elementary volume) have been made on plant fiber composites associated with epoxy, bio-epoxy, and polyester resin [10, 13], but also thermoplastic polymers of PLA [10, 14]. Many techniques exist to measure it at different scales [10, 15, 16]. The microscopic tests directly measure the shear strength of the interfacial shear strength (IFSS). The microscopic analysis has the advantage of directly evaluating the damage of the fiber–matrix interface. Several micromechanical techniques for the determination of interfacial shear stress exist, but they are very expensive:

1. The loosening of a fiber from a matrix pad [10, 17, 18]
2. The fragmentation of a unit fiber [10, 19–21]
3. Matrix microdrop dropout [22, 23]
4. Micro-indentation (push-out) [10, 24, 25].

Few studies describe the properties of the interfacial zone of biocomposites, while the improvement in mechanical performance requires a better understanding of this area [14, 22, 23]. The behavior of the fiber–matrix interface is very complex, and experimental tests are very expensive to determine the resistance interface and therefore a resistant material. It is necessary to provide a numerical model to understand the mechanical behavior of the interface in as much detail as possible in order to provide the experimenters with a very rich theoretical database. In our knowledge, there are no theoretical works which have treated and discussed the fiber–matrix interface damage of hybrid biocomposite jute–Alfa/PEEK and biocomposite materials jute/PEEK and Alfa/PEEK. In this context, our contribution consists in developing a numerical model based on genetic approach to study the effect of thermal stress on the fiber–matrix interface damage of three new hybrid biocomposite jute–Alfa/PEEK and biocomposite materials jute/PEEK and Alfa/PEEK. To determine the damage to the interface, we have used an analytical model based on Weibull probability formalism (fiber and

matrix damage) [26–30]. The objective function of our algorithm was based on the Cox mathematical model and Lebrun equation. The distance between fibers was determined by the concept of volume and mass fraction of reinforcement presented by Antoine [31, 32].

The characteristics of the materials used

The matrix PEEK

Given the wide range of thermoplastics, amorphous or semicrystalline, the choice of resin is made by eliminating the matrices that do not correspond to the specifications (Table 1). Indeed, to be used in a civil aircraft nacelle environment, they must meet the following specifications [33]:

- Maximum operating temperature greater than or equal to 120 °C
- Good mechanical properties (tensile modulus greater than 2 GPa, tensile strength greater than 100 MPa)
- Density less than 1.5
- Compatibility of the carbon reinforcement (thermal expansion of the matrix as low as possible to be close to that of carbon and thus avoid the formation of internal stress)
- Resistance to the environment: good resistance to wet aging, aeronautical fluids (solvents, kerosene, hydraulic fluid, etc.)
- Use of the PEEK matrix: semicrystalline thermoplastic.

Polyetheretherketone (PEEK) is a so-called thermostable thermoplastic polymer. Its macromolecular skeleton consists of benzene rings and ketone bonds (Fig. 2) which give it an excellent resistance to both thermal and chemical aggression (Fig. 2) [34].

Figure 3 shows the normalized density resistance for the thermosetting and thermoplastic matrices most used in the design of aeronautical parts based on their mass cost. It emerges that a thermoplastic, in particular the thermoplastic PEEK, could be an alternative solution for the manufacture of composite parts, in particular for aeronautical applications at high temperatures [34].

Fibers

Alfa fibers

The Alfa is well known for papermaking applications as a noble raw material; however, it is not known in textile applications, except for the realization of handicrafts for which the strands are used without treatment. It has also been a source of inspiration for making green composites (for orthopedic prosthesis

Table 1 The physical characteristics of the PEEK matrix [33, 36, 37]

Matrix	$T°$ max temperature continuous use (°C)	σ breaking (MPa)	Young's modulus (GPa)	Density (g/cm^3)	Glass transition temperature T_g (°C)	T_f melting temperature (°C)
PEEK	240	120–140	3.6	1.3	143	343

Fig. 2 The PEEK monomer

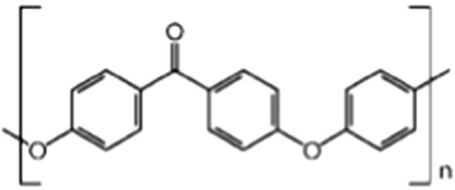

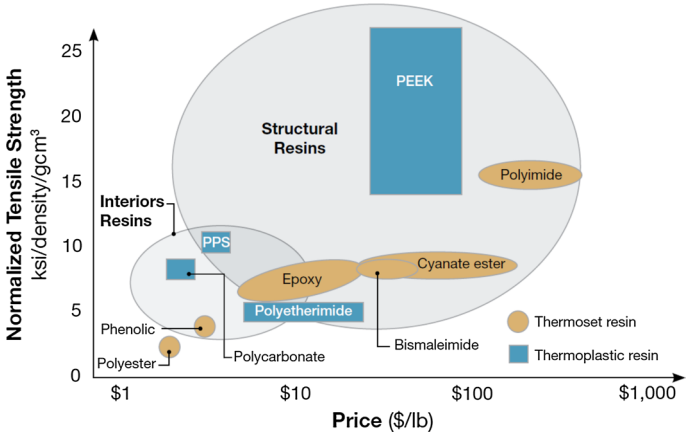

Fig. 3 Cost-effective mechanical resistance for large families of polymer matrices [34, 35]

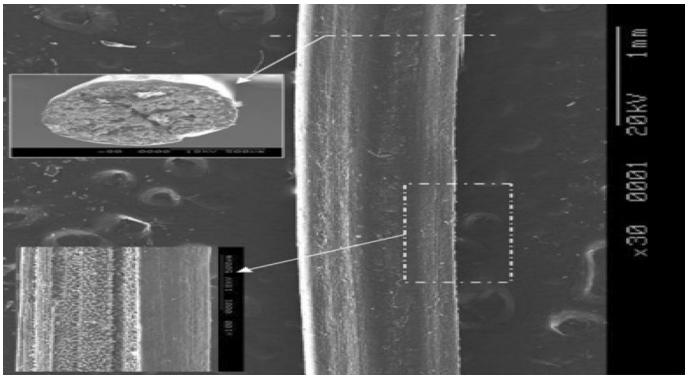

Fig. 4 SEM picture of untreated Alfa stem [38]

application) and has been used in combination with other natural fibers such as wool in the manufacture of nonwovens, but never for textile applications properly [4, 7, 38].

Figure 4 shows a SEM image of an untreated Alfa stem [38].

Figure 5 presents a SEM image of a facies of fracture of an Alfa fiber after a tensile test [38].

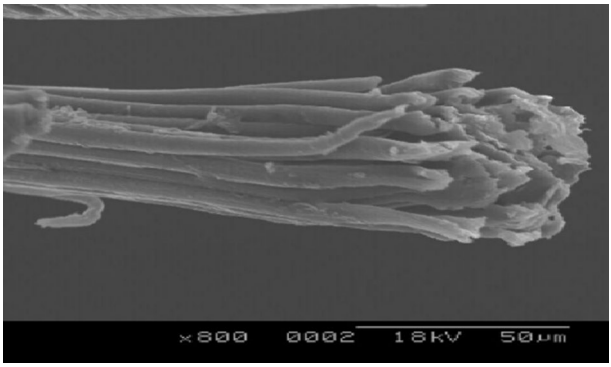

Fig. 5 SEM picture of a fracture facies of an Alfa fiber after a tensile test [38]

Jute fiber

The jute fiber is derived from the stem of the plant (Corchorus capsularis and Corchorus olitorius). It is mainly found in the humid tropics, and its production is in China (35,500 t, FAO 2014) and especially in India (1,940,000 t, FAO 2014) and Bangladesh (1,391,000 t, FAO 2014). This production makes it the second most important fiber produced after cotton. It is composed of 61–72% cellulose, 13.6–20% hemicellulose, and 11.8–13% lignin, and its mechanical properties are comparable to those of hemp. In addition, its fibers are long, 4 m, but provided with nodes. The fibrils possess a diameter of between 40 and 80 µm and an irregular lumen [39]. The coarser fibers are used as strings, wrapping, and carpets, where these fibers can compete with polypropylene [40], while the finer fibers can be mixed with wool, cotton [41], or other natural fibers to form fabrics; its moisture-absorbing capacity is an advantage. Jute is found in geotextile coatings as a source of raw materials in the paper industry. Jute fiber is also used in combination with soy protein for biodegradable composites [42, 43].

Figure 6 shows the SEM images of jute fibers (a) untreated, (b) alkali-treated, (c) bleached, (d) milled, (e) and (f) hydrolyzed with acid [44].

In our study, we used two types of natural reinforcements—Alfa and jute fibers—whose characteristics are mentioned in Table 2.

Mathematical models

The nonlinear acoustic technique

The classical nonlinear acoustic behavior of materials is commonly described by the addition of a nonlinear term β in Hooke's law, which is written as

$$\sigma = E\varepsilon(1 + \beta\varepsilon) \tag{1}$$

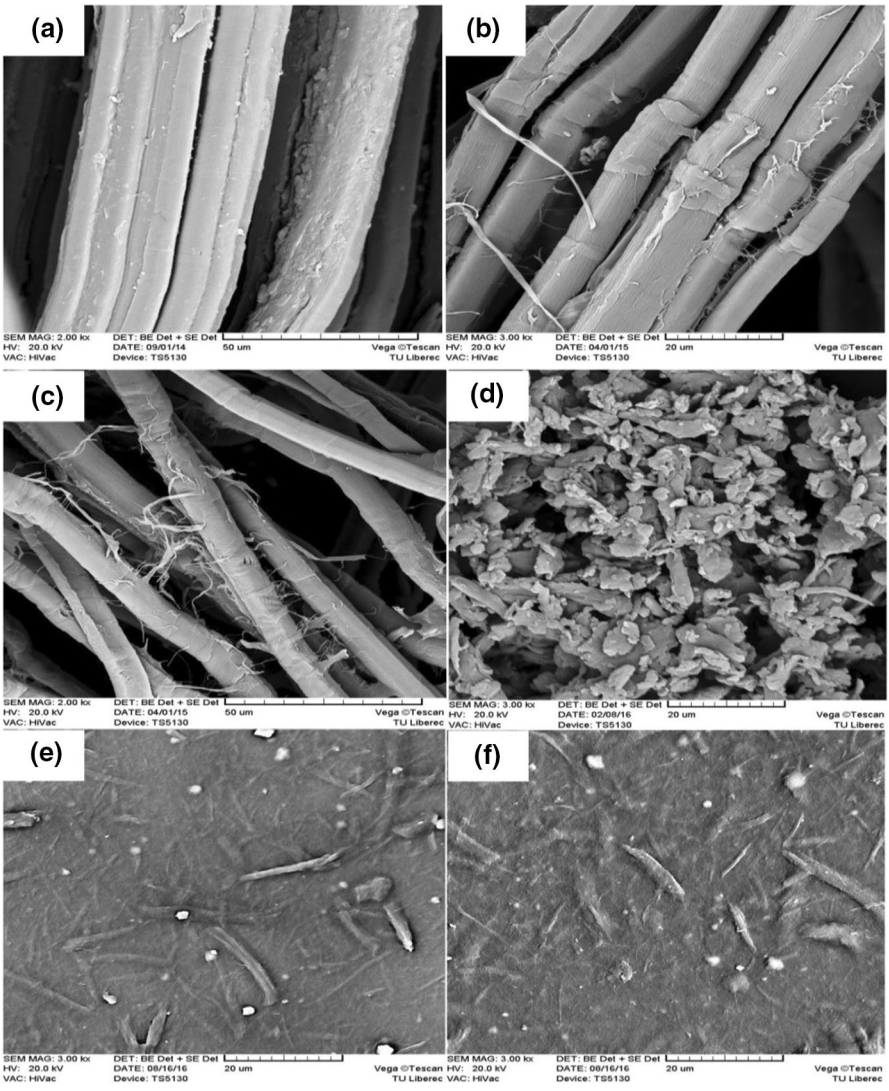

Fig. 6 SEM images of jute fibers **a** untreated, **b** alkali-treated, **c** bleached, **d** milled, **e** and **f** acid-hydrolyzed. "Reprinted with permission from Elsevier/Springer" [44]

In the last relation, σ and ε are the stress and strain, respectively [47–51], E is the Young's modulus, and β is the parameter of nonlinearity. If $\beta = 0$, we say that the material is homogeneous. E and β can be determined from acoustic measurements [52, 53]. The Young's modulus E is obtained by determining the rates of longitudinal and transverse propagation. The harmonic generation method is based on the distortion of a sine wave of a high intensity through a given material or medium. When the material does not exhibit heterogeneity, different areas excited by the ultrasonic agitation vibrate at the same speed, the ultrasonic wave

Table 2 The physical properties of the fibers used [38, 45, 46]

Fibers	Density (g/cm^3)	Length (mm)	Diameter (µm)	Cellulose (%)	Hemicellulose (%)	Lignin (%)	Maximum deformation in tension (%)	Young's modulus (GPa)	Absorption humidity (%)
Alfa	1.51	0.6–14	5–10	45	24	24	1–4	12.7	12
Jute	1.44	2.5	20	61.1–71.5	13.6–20.4	11.8–13	1.5–1.8	26.5	12

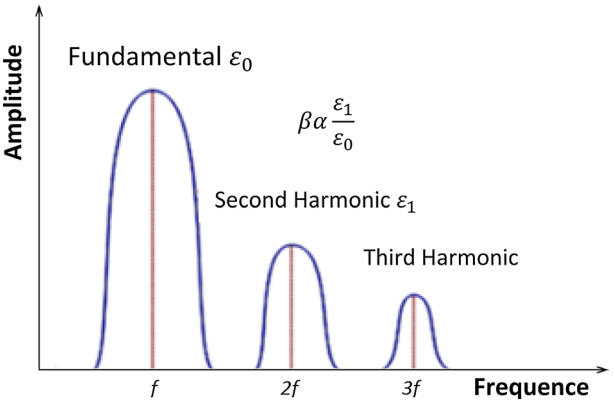

Fig. 7 Fourier spectrum of the received signal for nonlinear parameter determination

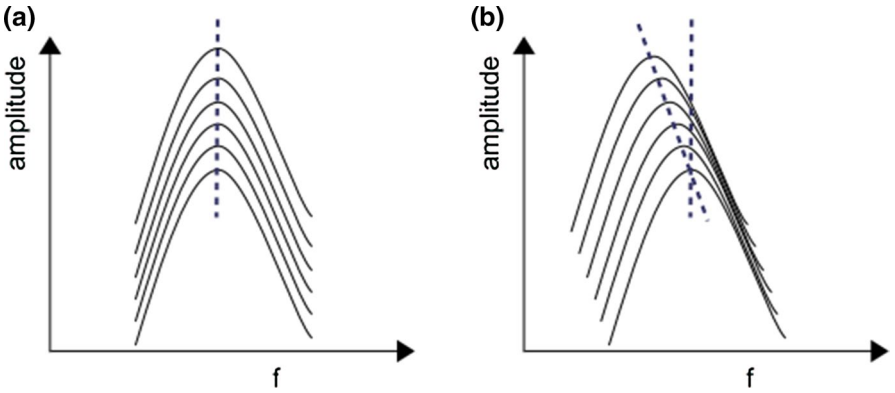

Fig. 8 Representation of the evolution of a resonance as a function of the excitation amplitude in an intact material **a** and damaged material **b** [60]

is then subjected to any perturbation and its shape is the same that is to say sinusoidal. The presence of heterogeneity in the medium is observed at the source of the local increase or decrease of the density and the modulus during compression or expansion respectively [52, 53]. This results in the change in the wave shape of the spectral content (FFT) (Fig. 7). As a result, the received wave is not sinusoidal but contains harmonics.

The resonance method (Figs. 8 and 9) consists in the resonance frequency shift and the modification of the quality factor of vibrating "bars" with the increase in the excitation amplitude [54–56]. The offset of the resonance frequency and the decrease in the quality factor are proportional to the amplitude of the wave. These observations were attributed to a hysteretic nonlinearity [57–59]

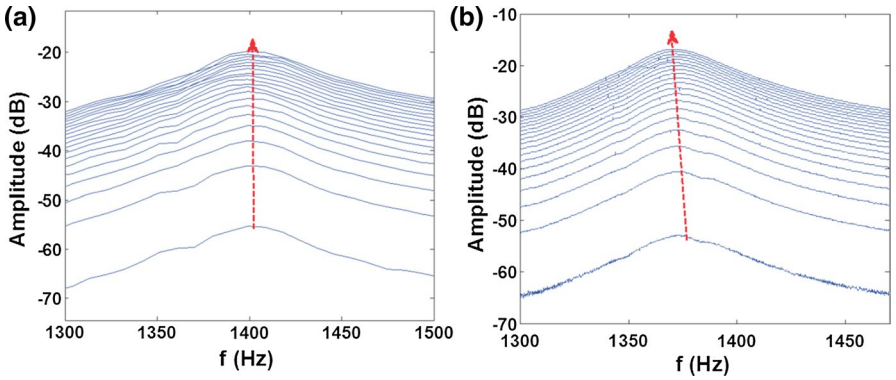

Fig. 9 Resonance spectra corresponding to a 2.5-mm-thick polymer matrix base in the intact state **a** and in the damaged state **b** (the resonance frequency of the damaged state is typically around 1380 Hz) [61]

Volume and mass fraction of reinforcement

In a composite, we write $V_f + V_m + V_v = 1$, where the subscripts f, m, and v relate, respectively, to the fibers, matrix, and porosity. In practice, V_f and V_v are mainly conditioned by the nature of the reinforcement, the matrix, and the method of implementation. The orders of magnitude are common [31]:

$$0.3 < V_f < 0.65$$

$$0.001 < V_v < 0.1$$

$$W_i = \frac{W_i}{W_c} \tag{2}$$

where W_i is the weight of component i and Wc is the total weight of the composite.

$$\sum_{i=1}^{N} W_i = 1 \tag{3}$$

The mass of the constituents of the composite is given by

$$W_c = \rho_c V_c;$$

$$W_f = \rho_f V_f;$$

$$W_m = \rho_m V_m,$$

with ρ_c : the density of composite; ρ_f : density of fiber; ρ_m : density of the matrix

The total mass of the composite is $\rho_c V_c = \rho_f V_f + \rho_m V_m$which allows to derive the density of the composite as follows:

$$\rho_c = \frac{\rho_f V_f + \rho_m V_m}{V_c} \tag{4}$$

Similarly, one can express the density as a function of mass fraction on the basis of the total volume of the composite $V_c = V_m + V_f$:

$$\rho_c = \frac{\rho_f V_f + \rho_m V_m}{V_m + V_f}$$

$$\rho_c = \frac{W_f + W_c}{\frac{W_f}{\rho_f} + \frac{W_m}{\rho_m}}$$

$$\rho_c = \frac{1}{\frac{W_f}{\rho_f} + \frac{W_m}{\rho_m}} \tag{5}$$

Thermal stress

The thermal stress field which results from the differential expansion of the fibers and the matrix during cooling after preparation of the composite at high temperature is given by the following equations: [62]

$$\sigma_f^t = E_f \frac{a}{1+a}\left(M_2 - M_0\right) \tag{6}$$

with

$$M_0(T) = \int_{T_0}^{T_e} \left(\alpha_m - \alpha_f\right) \mathrm{d}T$$

$$M_2(T) = \int_{T_e}^{T} \left(\alpha_m - \alpha_f\right) \mathrm{d}T$$

with T_0, the room temperature; T_e, the temperature of development; and T, the test temperature. α_f and α_m are the expansion coefficients of the fiber and matrix [62].

The formalism probabilist of Weibull

When the stress is uniform, damage to the matrix is given by Formula (7) of Weibull [29]:

$$D_{\mathrm{m}} = 1 - \exp\left\{-\frac{V_{\mathrm{eff}}}{V_0}\left(\frac{\sigma_{\mathrm{f}}}{\sigma_0}\right)^{m}\right\} \tag{7}$$

with (σ_{f}), the applied stress; (V_{eff}), the volume of the matrix; $(m$ and $\sigma_0)$, the Weibull parameters; and V_0, the initial volume of the matrix.

A broken fiber is discharged over its entire length. In other words, it can only break once. The rupture obeys a law similar to that described for the matrix; damage to the fiber is given by Eq. (8):

$$D_{\mathrm{f}} = 1 - \exp\left\{-A_{\mathrm{f}} \times L_{\mathrm{equi}} \times \left(\frac{\sigma^{\mathrm{f}}_{\mathrm{max}}}{\sigma_{0\mathrm{f}}}\right)^{m_{\mathrm{f}}}\right\} \tag{8}$$

with $\sigma^{\mathrm{f}}_{\mathrm{max}}$, the maximum stress applied to the fiber; $\sigma_{0\mathrm{f}}$, the initial stress applied to the fiber; m_{f}, the Weibull parameter; and $A_{\mathrm{f}} = \pi \times a^2$; L_{equi}, the length of the fiber at equilibrium.

The mathematical model of Cox

It is possible to describe the charge transfer processes by simplified micromechanical models considering, for example, a representative elemental volume (REV) consisting of a fiber embedded in a cylinder of matrix on which a tensile stress is applied. The writing of the equilibrium elastic equation theoretically makes it possible to determine the profile of the tensile stress in the fiber and that of shear at the interface. From these data, it is possible to evaluate the stress–strain curve of the composite [63] (Fig. 10).

Depending on the assumed behavior of the interface, different responses can be simulated. In the Cox model, the connection between fiber and matrix is assumed to be perfect and also the mechanical behavior of these elastic constituents [63].

For the interface, their damage based on the model of Cox [63] is defined by Eq. (9):

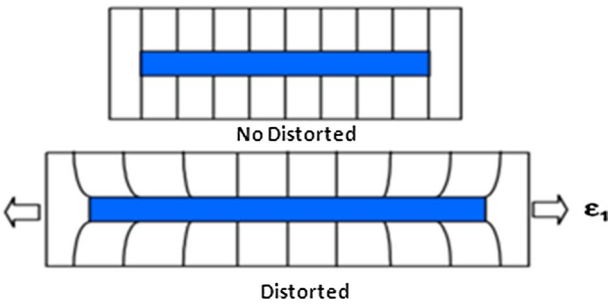

Fig. 10 Representative elemental volume (REV)

$$\tau = \frac{E_f \times a \times \varepsilon}{2} \beta \left(\tanh \left(\beta \times \frac{l}{2} \right) \right) \tag{9}$$

$$\beta = \frac{2G_m}{E_f \times r_f^2 \times \ln \left(\frac{R}{r_f} \right)}$$

with G_m, the shear modulus of the matrix; E_f, Young's modulus of the fiber; ε, the deformation; a, the radius of the fiber; R, the distance between fibers; τ, shear stress of the interface; and r_f, the distance between fiber and the matrix.

Modeling by genetic algorithm

The description of the implementation of the genetic model

In our genetic algorithm, the analytical model of Cox Eq. (9) and the Lebrun model Eq. (6) will be used to evaluate the objective function and to see the effect of the thermal stress on the damage to the interface of the three hybrid biocomposite and biocomposite materials. The damage of the fibers and the matrix will be calculated using the Weibull's Eqs. (7 and 8).

The interface damage is produced by the genetic operator crossing of the two damages of the constituents, fiber and matrix, using a mutation probability equal to 0.25. The found individuals are ranked and positioned to get the best of them, these individuals are inserted in the first row, and we have a new generation; the process is repeated until convergence (reach the maximum generation value Gmax). The applied tensile stress values are 90 N/m^2, 115 N/m^2, and 140 N/m^2. The Young's modulus for both fibers is shown in Tables 1 and 2. The numerical calculations are performed using the MATLAB platform.

We validate the results obtained by genetic modeling using the nonlinear acoustic technique Eq. (1); we have determined the different values of the nonlinear parameter β for the three biocomposite materials using Eq. (1).

The flowchart of our program

The principle of this algorithm is based on the use of genetic operators (selection, crossover, mutation) to predict a population of 320 randomly generated individuals with a maximum output of 160 as a stopping criterion. The chromosome genes represent the following variables defined by the analytical model of Cox: the mechanical stress, Young's modulus of the fiber, modulus of shear of the matrix, radii of the fibers, and the distance between fibers. The damage to the interface is calculated by the crossing of the two damages, fiber and matrix, using a mutation probability of 0.25.

In Fig. 11, we have presented the details of our genetic model which is developed with MATLAB platform.

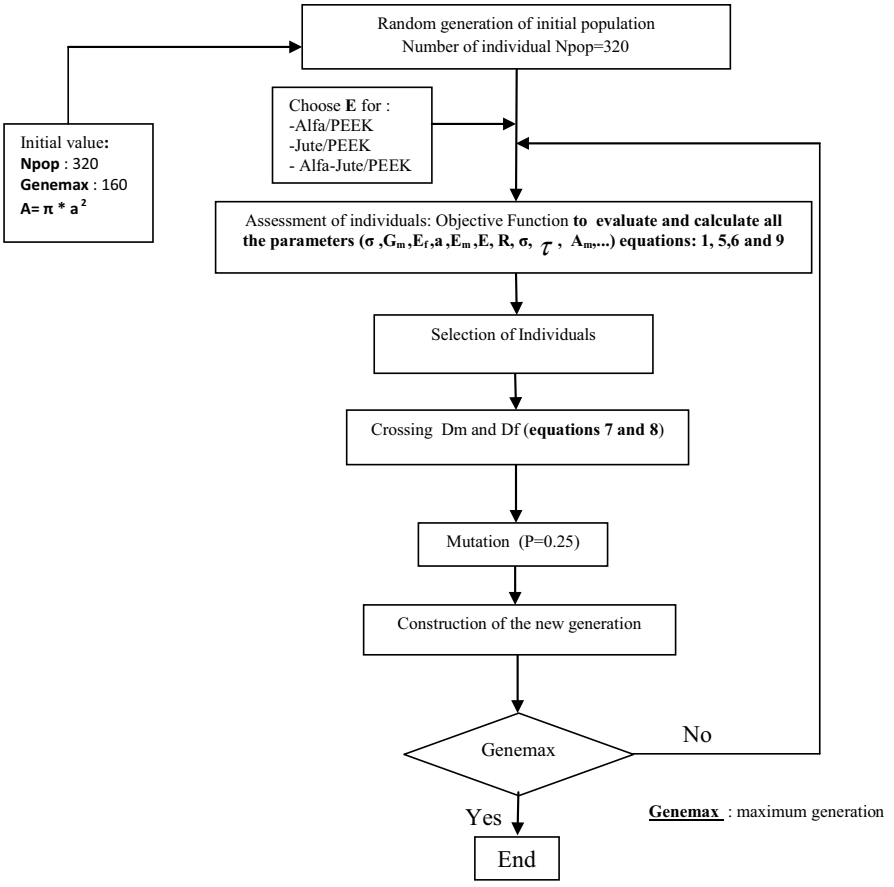

Fig. 11 The flowchart of our program

We define below the cc our genetic program:

Crossing function

```
function [enf1, enf2]=cross(p1,p2)
nbVar = length(p1);
enf1=[];
enf2=[];
a = rand;
enf1 = p1*a + p2*(1-a);
enf2 = p2*a + p1*(1-a);
return
```

Mutation function

```
function [enf1] = mutate(enf1,probMut)
bound=[10  1000];
[nbenf nbvr]=size(enf1);
df = bound(2) - bound(1);
for k=1:nbenf
a = rand;
if a < probMut
indiv = enf1(k,:);
mPoint = round(rand * nbenf);
if mPoint ~= 0
  L=round(3*rand);
 if L ~= 0
enf1(k,L) = bound(1)+ rand*df;
end
end
end
end
```

Discussion and interpretation of results

Our calculation was carried out on three types of hybrid biocomposite and biocomposite materials, Alfa/PEEK, jute/PEEK, and Alfa–jute/PEEK. Our genetic results have been presented in the figures by the blue cloud; the blue dots represent the fiber–matrix interface damage of the three hybrid biocomposite and biocomposite materials. We have examined the strength of our materials by the application of different mechanical tensile stress (90 N/m^2, 115 N/m^2, and

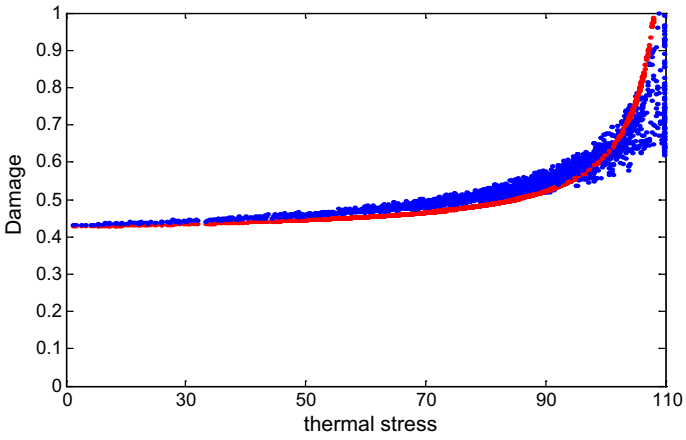

Fig. 12 The influence of the thermal stress on the damage of the interface for $\sigma = 140$ N/m^2

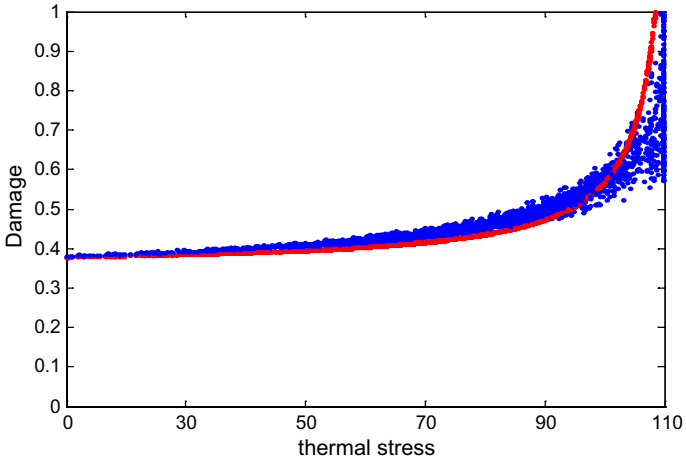

Fig. 13 The influence of the thermal stress on the damage of the interface for $\sigma = 115$ N/m^2

140 N/m^2) and this at 0 °C (thermal stress = 0), and we have observed the evolution of the damage to interface when the thermal stress is varied between 0 and 110 N/m^2; we have observed a rapid growth in the fiber–matrix interface damage for the three studied materials.

To validate our results, we have introduced the nonlinear parameter β in our algorithm. The results were presented by the red curve in all figures using Eq. 1.

Figures 12, 13, 14, 15, 16, 17, 18, 19, and 20 show the level of damage to the interface for the three materials as a function of thermal stress.

In Table 3, we presented all the values of the physico-mechanical parameters used in our calculation program.

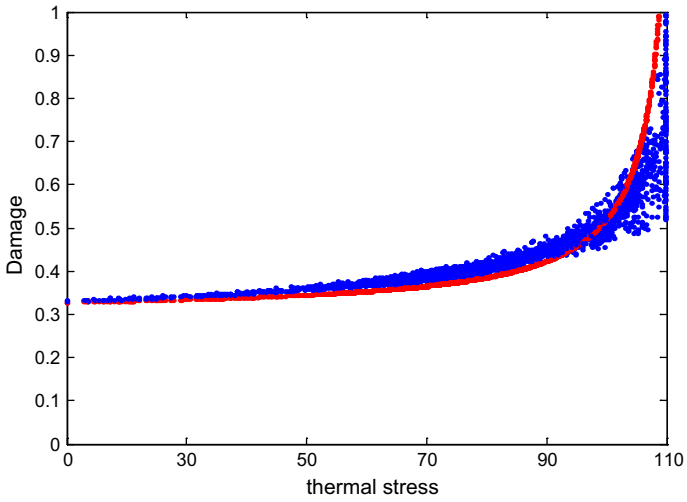

Fig. 14 The influence of the thermal stress on the damage of the interface for $\sigma = 90$ N/m^2

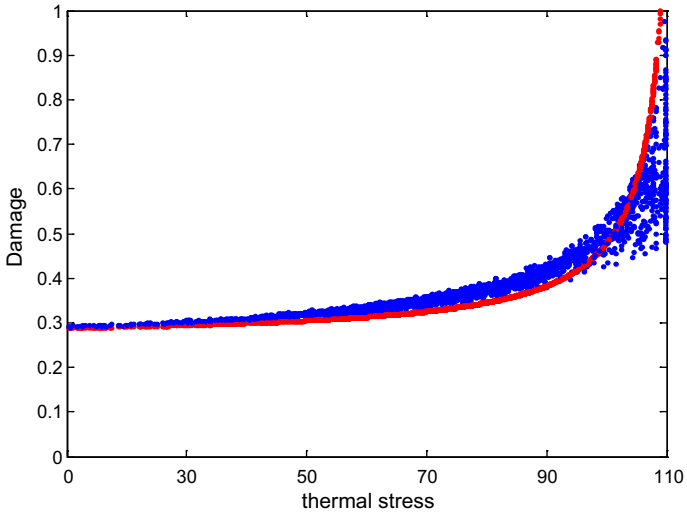

Fig. 15 The influence of the thermal stress on the damage of the interface for $\sigma = 140$ N/m^2

Jute/PEEK

Figures 12, 13, and 14 show that the damage "*D*" of the interface starts at the level of 0.325 on (90 N/m^2) and then increases to a maximum value of 0.425 for (140 N/m^2) before the application of the thermal stress; we observed that when the thermal stress increases, the damage of the interface of the jute/PEEK increases and reaches its maximum of 0.7 for a value of the thermal stress 95 N/m^2. It can also be said that

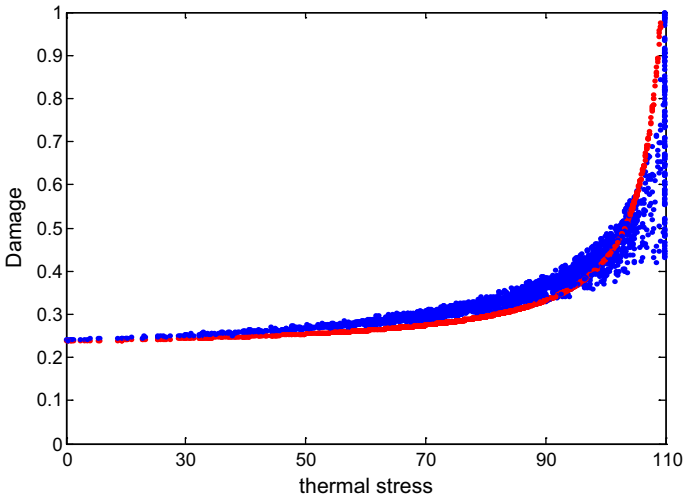

Fig. 16 The influence of the thermal stress on the damage of the interface for $\sigma = 115$ N/m^2

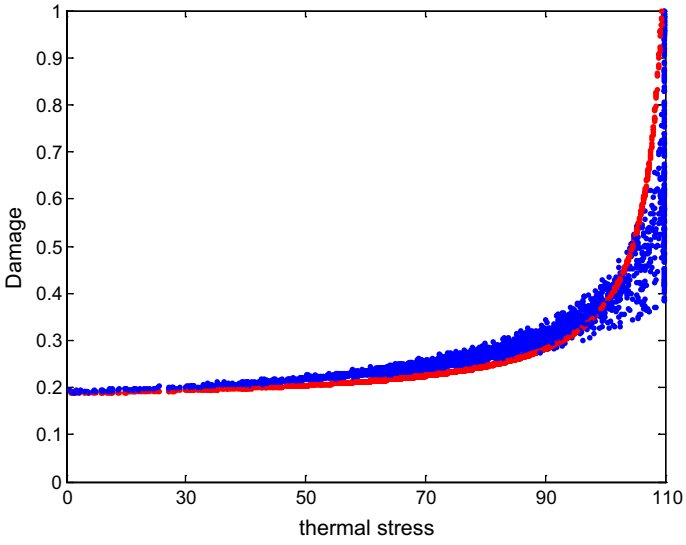

Fig. 17 The influence of the thermal stress on the damage of the interface for $\sigma = 90$ N/m^2

the increase in the thermal stress affects and gives a strong degradation to the interface by comparing with the applied mechanical stress.

Alfa/PEEK

Figures 15, 16, and 17 show that the damage "*D*" of the interface starts at the level of 0.2 on (90 N/m^2) and then increases to a maximum value of 0.31 for (140 N/

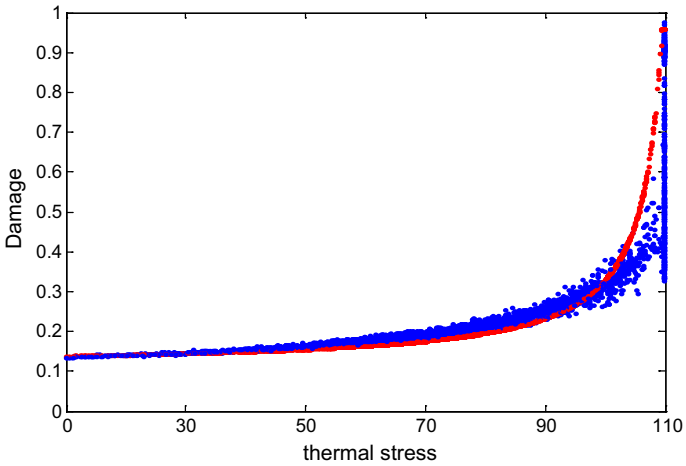

Fig. 18 The influence of the thermal stress on the damage of the interface for $\sigma = 140$ N/m^2

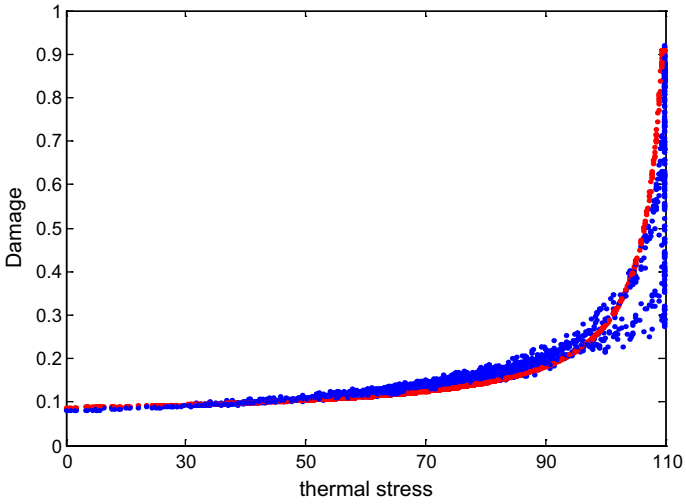

Fig. 19 The influence of the thermal stress on the damage of the interface for $\sigma = 115$ N/m^2

m^2) before the application of the thermal stress; we observed that when the thermal stress increases, the damage of the interface of the jute/PEEK increases and reaches its maximum of 0.45 for a value of the thermal stress of 95 N/m^2. It can also be said that the increase in the thermal stress affects and gives a strong degradation to the interface by comparing with the applied mechanical stress. The results show that the Alfa/PEEK interface is more resistant to thermal and mechanical stress compared with the jute/PEEK interface.

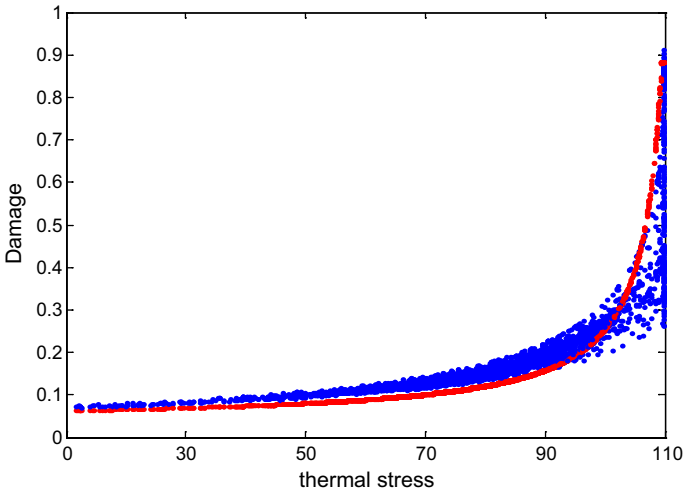

Fig. 20 The influence of the thermal stress on the damage of the interface for $\sigma = 90$ N/m^2

Table 3 The values of the physico-mechanical parameters used in our calculation program

Materials	PEEK	Jute	Alfa
Young's modulus (GPa)	3.6	26.5	12.7
Density (g/cm^3)	1.3	1.44	1.51
Diameter (μm)	–	8.0	8.0
Length (mm)	–	20	20
Thermal stress	0–110	0–110	0–110
Tensile stress	90–140	90–140	90–140
Coefficient of thermal expansion α_i (1/C°)	0.021×10^{-5}	1.9×10^{-5}	1.9×10^{-5}
Weibull parameters (m)	1.2	1.3	1.3
Distance between fibers R (μm)	12		

Alfa–jute/PEEK

Figures 18, 19, and 20 show that the damage "D" of the interface starts at the level of 0.05 on (90 N/m^2) and then increases to a maximum value of 0.125 for (140 N/m^2) before the application of the thermal stress; we observed that when the thermal stress increases, the damage of the interface of the jute/PEEK increases and reaches its maximum of 0.21 for a value of the thermal stress of 95 N/m^2. It can also be said that the increase in the thermal stress affects and gives a strong degradation to the interface by comparing with the applied mechanical stress. The results show that the interfaces of biocomposites hybrid Alfa–jute/PEEK are more resistant to thermal and mechanical stress compared with the jute/PEEK and Alfa/PEEK biocomposite materials.

Our genetic results are in very good agreement with the results obtained by the nonlinear acoustic technique which presents the fiber–matrix interface damage by the graphs in red.

In our knowledge, there are no theoretical works which have treated and discussed the fiber–matrix interface damage of the three hybrid biocomposite and biocomposite materials, and in order to validate our results, we have used the analytical model of the nonlinear acoustic technique given by Eq. (1). The results of this model were presented by the figures in red color. These results are similar and agree very well with our results found by genetic simulation presented by the blue cloud. The experimental work presented by Antoine Le Duigou et al. at different scales [14, 22, 23, 65, 66] and the work of Bodros et al. [64] have shown that the use of natural fibers greatly improves the mechanical properties of composite materials and also they have a very low environmental impact.

Conclusion

In this theoretical work, we have studied the influence of thermal stress on the fiber–matrix interface damage of the three hybrid biocomposite and biocomposite materials (jute/PEEK, Alfa/PEEK, and Alfa–jute/PEEK). The results of our genetic simulation show that the hybrid biocomposite Alfa–jute/PEEK is more resistant to mechanical and thermal stress compared with the other two biocomposite materials and that the biocomposite Alfa/PEEK materials are much more resistant to the same constraints applied and with the same volume fraction as biocomposite jute/PEEK, and this is mainly due to the fact that Alfa fiber contains twice as much hemicellulose and lignin as jute fiber. Our genetic results are in very good agreement with the results obtained by the nonlinear acoustic technique and the real behavior of the three materials as well as the results obtained in our modeling are in good agreement with the experimental results found by Antoine Le Duigou et al. which showed that the biocomposites have better physical and mechanical properties and are stronger than composite materials and also they have a very low environmental impact.

Acknowledgements The authors acknowledge the financial support from the General Direction of Scientific Research and Technological Development of the Ministry of Higher Education and Scientific Research of Algeria.

References

1. Fowler Paul A, Hughes J, Elias Mark, Robert M (2006) Bio-composites: technology, environmental credentials and market forces. J Sci Food Agric 86(12):1781–1789
2. Ariadurai S (2013) Bio-composites: current status and future trends. The Open University of Sri Lanka, Nawala, p 2013
3. Vogüé A (1927) Notes sur la culture et la production du Jute. Revue de botanique appliquée et d'agriculture coloniale 7:447–461
4. Med Ben Ali A, Bencheikh R, Vermeulen B, Perwuelz A, Chaker A (2006) Réalisation d'un nontissé à base de fibres végétales d'alfa, 2ème Congrès International de la Recherche Appliquée en Textile (Cirat 2) Monastir, Tunisie

5. Michud A, Giustini B (2009) Les fibres cellulosiques à usage textile. Mémoire, Cellule de veille technologique de Grenoble INP-Pagora, École internationale du papier, de la communication imprimée et des biomatériaux
6. Feughelman M (1997) Mechanical properties of wool fibers & the two-phase model », Mechanical properties and structure of alpha-keratin fibers: wool, human and related fibers. University of New South Wales Press, Randwick, pp 28–59
7. Ben Brahim S, Ben Cheikh R (2007) Influence of fiber orientation and volume fraction on the tensile properties of unidirectional Alfa-polyester composite. Compos Sci Technol 67(1):140–147. https://doi.org/10.1007/s00289-020-03183-7
8. Boughriet R (2009) Fibres végétales : de nouvelles applications prometteuses émergent. www.Actu-Environnement.com
9. Casey R, Grove C (1947) Fibers. J Ind Eng Chem 39(10):1213–1215
10. Gourier C (2016) Contribution à l'étude de matériaux biocomposites à matrice thermoplastique polyamide-11 et renforcés par des fibres Lin. Thèse de doctorat, Université de Bretagne Sud
11. Fuentes CA, Tran LQN, Van Hellemont M, Janssens V, Dupont-Gillain C, Van Vuure AW et al (2013) Effect of physical adhesion on mechanical behaviour of bamboo fibre reinforced thermoplastic composites. Colloid Surf A 418:7–15
12. Thomason J, Yang L (2013) Temperature dependence of the interfacial shear strength in glass reinforced polypropylene and epoxy composites
13. Marrot L, Bourmaud A, Bono P, Baley C (2014) Multi-scale study of the adhesion between flax fibers and biobased thermoset matrices. Mater Des 62:47–56
14. Le Duigou Antoine, Davies P, Baley C (2010) Macroscopic analysis of interfacial properties of Flax/PLLA biocomposites. Compos Sci Technol 70:1612–1620
15. Hodzic A, Kim JK, Stachurski ZH (2001) Nano-indentation and nano-scratch of polymer/glass interfaces. II: model of interphases in water aged composite materials. Polymer 42:5701–5710
16. Lee SH, Wang S, Pharr GM, Xu H (2007) Evaluation of interphase properties in a cellulose fiber reinforced polypropylene composite by nanoindentation and finite element analysis. Compos A Appl Sci Manuf 38:1517–1524
17. Stamboulis A, Baillie C, Schulz E (1999) Interfacial characterisation of flax fibre-thermoplastic polymer composites by the pull-out test. Die Angewandte Makromolekulare Chemie 272:117–120
18. Yang L, Thomason JL (2012) Development and application of micromechanical techniques for characterising interfacial shear strength in fibre-thermoplastic composites. Polym Test 31:895–903
19. Joffe R, Andersons J, Wallström L (2003) Strength and adhesion characteristics of elementary flax fibres with different surface treatments. Compos A Appl Sci Manuf 34:603–612
20. Huber T, Müssig J (2008) Fibre matrix adhesion of natural fibres cotton, flax and hemp in polymeric matrices analyzed with the single fibre fragmentation test. Compos Interfaces 15:335–349
21. Awal A, Cescutti G, Ghosh SB, Müssig J (2011) Interfacial studies of natural fibre/polypropylene composites using single fibre fragmentation test (SFFT). Compos A Appl Sci Manuf 42:50–56
22. Le Duigou Antoine, Baley C, Grohens Y, Davies P, Cognard J-Y, Créach'cadec R et al (2014) A multi-scale study of the interface between natural fibres and a biopolymer. Compos A Appl Sci Manuf 65:161–168
23. Le Duigou Antoine, Kervoelen A, Le Grand A, Nardin M, Baley C (2014) Interfacial properties of flax fibre–epoxy resin systems: existence of a complex interphase. Compos Sci Technol 100:152–157
24. Netravali A, Stone D, Ruoff S, Topoleski L (1989) Continuous micro-indenter push-through technique for measuring interfacial shear strength of fiber composites. Compos Sci Technol 34:289–303
25. Zhandarov S, Mäder E (2005) Characterization of fiber/matrix interface strength: applicability of different tests, approaches and parameters. Compos Sci Technol 65:149–160
26. Baxevanakis C (1994) Statistical behavior of laminated composites at failure. Thèse, Ecole des Mines de Paris
27. Harlow DG, Phoenix SL (1978) The chain of bundles probability model for the strength of fibrous materials 1: analysis and conjectures. J Compos Mater 12:195–213
28. Scop PM, Argon AS (1967) Statistical theory of strength of laminated composites. J Compos Mater 1:92–99
29. Weibull W (1939) A statistical theory of the strength of materials. R Swedish Acad Engl Sci Proc 151:1–45

30. Mokaddem A, Alami M, Boutaous A (2012) A study by a genetic algorithm for optimizing the arrangement of the fibers on the damage to the fiber–matrix interface of a composite material. J Tex Inst 103(12):1376–1382
31. Chateauminois A (2000) Cours Matériaux composites: descrisption microstructure d'un composite. https://fr.scribd.com/document/215287303/Microstructure. Accessed Feb 2019
32. Mokaddem A, Alami M, Temimi L, Boutaous A (2012) Effect of heat stress on the damage of the fibre matrix interface of a composite material (T300/914) by a genetic algorithm. Fibres Text East Europe 20(6):98–101
33. Jérémie A (2009) Etude comparative du comportement composites à matrice thermoplastique ou thermodurcissable. Autre. INSA de Rouen. Français. NNT: 2009ISAM0012
34. Borgna T (2017) Etude des propriétés de composite à matrice thermoplastique thermostable au delà de leur température de transition vitreuse. Thèse de doctorat à l'Université de Pau et des Pays de l'Adour, p 196
35. Red C (2014) The outlook for thermoplastics in aerospace composites. 2014–2023. In: High-performance composites, Gardner Business Media, Inc., Cincinatti, p 54–63
36. Chevalier N (2008) Projet TOUPIE cahier des charges matériau et sélection matériau, rapport n°DITT-08-0248
37. Walther BM (1998) An investigation of the tensile strength and stiffness of unidirectional polymer-matrix, carbon-fiber composites under the influence of elevated temperatures. In: Master's Thesis in engineering science and mechanics, Virginia Polytechnic Institute and State University
38. Mohamed D (2012) Evaluation du potentiel textile des fibres d'Alfa (*Stipa Tenacissima* L.) caractérisation physico-chimique de la fibre au fil. Thèse de Doctorat. Université de Haute Alsac e-Mulhouse
39. Hinrichsena ACKG (1991) Processing and characterization of jute fiber reinforced thermoplastic polymers. Polym Plast Technol Eng 30:5–6
40. Muthu SS, Gardetti M (2016) Sustainable fibres for fashion industry, N°2, vol 103. Springer, Singapore
41. Hassan ABSK, Sreenath V, Yang W, Mahendra M, Gharia T, Jeffries W (1996) Enzymatic polishing of jute/cotton blended fabrics. J Ferment Bioeng 81(1):18–20
42. Behera AK, Avancha S, Basak RK, Sen R, Adhikari B (2012) Fabrication and characterizations of biodegradable jute reinforced soy based green composites. Carbohydr Polym 88(1):329–335
43. Richard C (2018) Caractérisation chimique des fibres d'asclépiade et l'effet de différents traitements sur son comportement. SCA 730 Activité de recherche à l'Université de Sherbrooke, faculté de génie mécanique, p 112
44. Jabbar A, Militký J, Wiener J, MadhukarKale B, Ali U, Rwawiire S (2017) Nanocellulose coated woven jute/green epoxy composites: characterization of mechanical and dynamic mechanical behavior. Compos Struct 161(1):340–349
45. Taj S, Munawar M, Ali Khan S (2007) Natural fiber-reinforced polymer composites. Proc Pakistan Acad Sci 44(2):129–144
46. Paiva MC, Ammar I, Campos AR, Cheikh RB, Cunha AM (2006) Alfa fibres: mechanical, morphological and interfacial characterization. Compos Sci Technol 67:1132–1138
47. Doumi B, Mokaddem A, Benrekaa N, Alami M, Beldjoudi N, Boutaous A (2015) Simulation by a genetic algorithm and location by the non-linearacoustic technique of the shear damage to the fiber-matrix interface of a hybrid composite material alfa-carbon/epoxy. J Hybrid Mater De Gruyter 2015(2):10–16. https://doi.org/10.1515/hyma-2015-0002
48. Johnson PA, McCall KR (1994) Observation and implications of nonlinear elastic wave response in rock. Geophys Res Lett 21(3):165–168
49. Moussatov A, Castagnède B, Gusev V (2001) Observation of nonlinear interaction of acoustic waves in granular materials: demodulation process. Phys Lett A 283:216–223
50. Nagy PB (1998) Fatigue damage assesment by nonlinear ultrasonic material characterization. Ultrasonics 36:375
51. El Guerjouma R, Goujon I, Nachad H, Faiz A, Godin N, Bentahar M, Baboux JC (2002) Linear and non linear ultrasonics for material damage evaluation and health monitoring. Matériaux Tech 90:48–50
52. Van Den Abeele KE (1996) Elastic pulsed wave propagation in media with second or higher-order nonlinearity. Part I. Theoretical framework. J Acoust Soc 99(6):3334–3345
53. Van Den Abeele K, Johnson PA (1996) Elastic pulsed wave propagation in media with second or higher-order nonlinearity. Part II. Simulation of experimental measurement on berea sandstone. J Acoust Soc 99(6):3346–3352

54. Zheng Y, Maev RG, Solodov IY (1999) Nonlinear acoustic applications for materials characterization. Can J Phys 77:927–967
55. Ostrovsky LA, Johnson PA (2001) Dynamic nonlinear elasticity of geomaterial. Rivista del Nuevo Cimento 24:1–46
56. Nazarov VE, Ostrovsky LA, Soustova IA, Sutin A (1998) Nonlinear acoustics of micro-inhomogeneous media. Phys Earth Planet Int 50:65–73
57. Bruneau M, Potel C, (2006) Matériaux et Acoustique 2, ch. 2. Hermès Science Publication, Lavoisier
58. Granato AV, Luke K (1966) The vibrating string model of dislocation damping. Phys Acoust Princ Methods 4:120
59. Nowick AS (1950) Variation of amplitude-dependent interval friction in single crystal copper with frequency and temperature. Phys Rev 80:249–257
60. Marec A (2008) Contrôle de santé des matériaux hétérogenes par émission acoustique et acoustique non linéaire: Discrimination des mécanismes d'endommagement et estimation de la durée de vie restante. Thèse de doctorat à l'école Doctorale de l'Université du Maine, Le Mans, p 138
61. Baccouche Y (2013) Caractérisation non linéaire de l'endommagement des matériaux composites par ondes guides. Université du Maine, 2013. Français. NNT: 2013. LEMA1011
62. Lebrun GA (1996) Comportement thermomécanique et durée de vie de composites à matrice céramique: théorie et expérience, Thèse de Doctorat n° 1606, Université de Bordeaux
63. Cox HL (1952) The elasticity and strength of paper and other fibrous materials. Br J Appl Phys 12:72–79
64. Bodros E et al (2007) Could biopolymers reinforced by randomly scattered flax fibre be used in structural applications? Comput Sci Technol 67(3–4):462–470
65. Le Duigou Antoine et al (2008) Effect of recycling on mechanical behaviour of biocompostable flax/poly (L-lactide) composites. Compos Part A 39(9):1471–1478
66. Le Duigou A, Davies P, Baley C (2009) Etude de la liaison interfaciale fibre de lin/acide poly (L-lactique) = study of interfacial bonding of flax fibre/poly (L-lactide). JNC 16, Toulouse, France. AMAC. hal-00388871